

Design Optimization for Plasma Control and Assessment of Operation Regimes in JT-60SA

T. Fujita 1), H. Tamai 1), M. Matsukawa 1), G. Kurita 1), J. Bialek 2), N. Aiba 1), K. Tsuchiya 1), S. Sakurai 1), K. Hamamatsu 1), N. Hayashi 1), N. Oyama 1), T. Suzuki 1), G.A. Navratil 2), Y. Kamada 1), Y. Miura 1), Y. Takase 3), D. Campbell 4), J. Pamela 5), F. Romanelli 6), M. Kikuchi 1)

1) Japan Atomic Energy Agency, Naka, Ibaraki-ken 311-0193, Japan

2) Columbia University, New York, NY 10027, USA

3) The University of Tokyo, Kashiwa, Chiba-ken 277-8561, Japan

4) EFDA, Germany

5) EFDA JET, UK

6) ENEA, Italy

E-mail contact of main author: fujita.takaaki@jaea.go.jp

Abstract. Design of modification of JT-60U, the JT-60SA device, has been optimized in viewpoint of plasma control, and operation regimes have been evaluated. Divertors with different geometry are prepared for flexibility of plasma shape control. The beam lines of negative-ion NBI are shifted downward for off-axis current drive, in order to obtain a weak/reversed shear. The feedback control coils along the port hole in the stabilizing plate are found to effective to suppress the resistive wall mode (RWM) and sustain high β_N close to the ideal wall limit. The regime of full current drive operation has been extended with upgraded heating and current drive power. Full current drive operation for 100 s with reactor-relevant high values of normalized beta and bootstrap current fraction ($I_p = 2.4$ MA, $\beta_N = 4.4$, $f_{BS} = 0.70$, $\bar{n}_e/n_{GW} = 0.86$, $HH_{y2} = 1.3$) is expected in a highly-shaped low-aspect-ratio configuration ($A = 2.65$).

1. Introduction

JT-60SA, modification of JT-60U, is a tokamak with superconducting magnets that will be build in the present JT-60U torus hall [1,2]. Many components of the present JT-60U facility including heating and current drive (CD) systems and power supply will be utilized. The plasma major radius is about 3 m, and a break-even-class high-temperature plasma is expected. The device is characterized by enhanced flexibility in the aspect ratio (A) and the plasma shape [1, 2]. The heating and current drive system has been upgraded to make total power of 41 MW available for 100 s [2-4], compared to 15 MW for 100 s (25 MW for 50 s) in the previous design. The system consists of 24 MW (85 keV) neutral beam injection (NBI), (perpendicular 16 MW, co-tangential 4 MW and counter-tangential 4 MW), 10 MW (500 keV) co-tangential negative-ion NBI (N-NBI), and 7 MW (110 GHz and 140 GHz) ECRF. Note that the tangential units of P-NB are balanced, while all 4 units (8 MW) were in the co-direction in the previous design.

This paper describes design optimization in JT-60SA in viewpoint of plasma control and plasma physics, and also describes evaluation of operation regimes. Poloidal field coils and divertor geometry for plasma shape control will be discussed in section 2. Section 3 presents optimization of ECRF and N-NB systems for heating and current drive. Resistive wall mode (RWM) control coils will be discussed in section 4. Section 5 describes expected operation regimes.

2. Plasma shape control

The flexibility in shape parameters such as elongation κ and triangularity δ and in the aspect ratio A is one of important features in JT-60U modification [1]. A configuration with a similar

shape and an aspect ratio to those for ITER ($A = 3.1$, $\kappa_{95} = 1.7$, $\delta_{95} = 0.33$, $S \sim 4.2$) and a configuration with strong shaping and a low aspect ratio ($A = 2.6$, $\kappa_{95} = 1.8$, $\delta_{95} = 0.5$, $S = 6.8$), which is believed to be suitable for high beta operation, are both possible [2]. Here, κ_{95} is the elongation of the 95% flux surface, δ_{95} is the triangularity of the 95% flux surface, and S is the shape parameter defined by $S = q_{95}I_p/aB_t$ [5], where q_{95} is the safety factor at the 95% flux surface, I_p is the plasma current, a is the plasma minor radius and B_t is the toroidal field at the plasma center.

The positions of poloidal (equilibrium) field coils have been changed from those for NCT-2 to make a space around the equator plane for maintenance and off-axis N-NB injection, the latter of which will be discussed in detail in section 3.2. This modification tends to enhance the triangularity and reduce the 'squareness' [6] of the plasma shape, which has a possibility to degrade the shape controllability especially in the low and medium δ regime including the ITER-like configuration. Hence we have decided to add one small equilibrium coil 'EF7' near the equator plane to enhance the shape controllability. This coil will be located above the equator plane to leave a space for off-axis N-NB injection below the equator plane.

The divertor geometry had not been fixed in considering available configurations in the previous study. A divertor geometry, at least one for an initial operation phase, needs to be determined before detail design work. Flexibility in the plasma configuration and the divertor performance are both taken into account for deciding the divertor geometry. Namely, a closed divertor configuration, like ITER, is preferable for enhanced divertor performance, though it restricts the location of the X point and hence the flexibility of configuration. The installation of divertor cassette [4, 7] for the remote handling maintenance has reduced the available space for the plasma. The structure of the divertor cassette has been optimized to keep κ , δ and S as high as possible.

Since JT-60SA is equipped with upper and lower divertors, we can employ different geometry for these two. The upper one has been optimized for high δ configuration, while the lower has been optimized for a wider range in the shape control including the ITER-like shape. This choice, not the reverse one (lower divertor for high δ), has been made for the off-axis CD with N-NB for high beta plasmas and for on-axis heating with N-NB for high-density H-mode experiments in the ITER-like shape as described later. Examples of typical plasma configurations are shown in Fig. 1. Figure 1 (a) shows a upper-single-null (USN) configuration with $I_p = 5.5$ MA,

$B_t = 2.7$ T, $q_{95} = 3.4$, $A = 2.65$, $\kappa_{95} = 1.74$, $\delta_{95} = 0.41$ and $S = 5.98$. Figure 1 (b) shows a lower-single-null (LSN) configuration with $I_p = 3.5$ MA, $B_t = 2.6$ T and $q_{95} = 3.0$. The aspect ratio and the shape parameters are $A = 3.10$, $\kappa_{95} = 1.71$, $\delta_{95} = 0.33$ and $S = 4.4$, which are nearly equal to those for ITER. In both configurations, both inner and outer hit points are located beneath the pumping slots for efficient divertor pumping. The configuration shown in Fig. 1 (a)

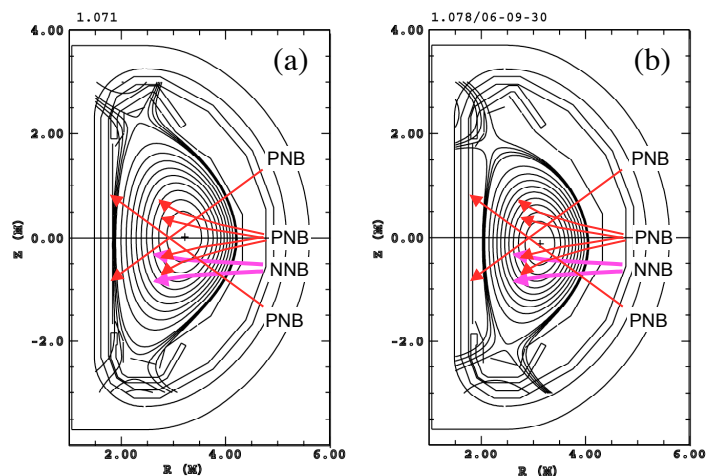


Fig. 1. Examples of plasma configuration with neutral beam lines. (a) Low A , highly shaped configuration. (b) ITER-like configuration.

has a higher κ_{95} and S than the double null (DN) configuration with four hit points beneath the pumping slots ($S \sim 5.5$). In Fig. 1, flux surfaces in the scrape-of-layer (SOL) regions are also shown for those which are located 1, 2, and 3 cm from the last closed flux surface on the outer equatorial plane. In Fig. 1 (a), the 1 cm SOL field line connects inner and outer target plates without intersecting other places including the baffle plates, while the 2cm SOL field line intersects the lower dome and inner baffles. In Fig. 1 (b), 1 and 2 cm SOL field lines connects inner and outer target plates, while the 3 cm SOL field line is open. Power from the plasma for 100 s 41 MW heating can be safely removed in these configuration, and the efficient particle control with divertor pumping is expected in the configuration shown in Fig. 1 (b).

3. Optimization of heating and current drive systems

JT-60SA will have P-NB, N-NB and EC as heating and current drive systems. Since the deposition region for P-NB moves near the plasma surface due to beam attenuation in the high-density regime, N-NB and EC are important for on-axis heating source in a high-density regime. This is one of the reasons for upgrade of power of N-NB and EC in the recent design.

3.1. ECRF system

The frequency of present EC systems in JT-60U is 110 GHz. The resonance toroidal field is 3.9 T for fundamental resonance and 1.95 T for second harmonic resonance for perpendicular injection (no Doppler shift). Since no effective heating is expected for the maximum toroidal field (2.73 T at $R = 3.00$ m) in the present JT-60SA design, change of frequency is considered. We have decided to use the 2nd harmonic resonance of higher frequency waves, since the cut-off of the wave can be met for high-density operation ($\sim 1 \times 10^{20} \text{ m}^{-3}$) if the fundamental resonance of lower frequency wave is used. We have selected 140 GHz, the gyrotron at which frequency is already developed. The cut-off density is $1.2 \times 10^{20} \text{ m}^{-3}$ for the 2nd harmonic EC resonance of a 140 GHz wave. The resonance location for perpendicular injection (no Doppler shift) is shown in Fig. 2. The deposition of EC depends on the toroidal magnetic field B_t . As B_t is reduced from 2.7 T, the resonance location moves inward (high-field side), and it jumps to the plasma surface on the low-field side when the higher order resonance radius enters into the plasma. The absorption fraction for 3rd harmonic resonance is 80% for the electron density $n_e = 2 \times 10^{19} \text{ m}^{-3}$ and the electron temperature $T_e = 3 \text{ keV}$, and hence the wave will be sufficiently absorbed at the 3rd resonance even in the peripheral region at least in H-mode plasmas.

One problem is that the current drive efficiency is quite low for the 3rd resonance since the absorption of waves injected obliquely takes place on both the high-field side and low-field side of the cold resonance radius due to weaker absorption than the 2nd resonance or fundamental resonance. Hence the ECCD by 140 GHz waves is only effective in the high B_t region ($B_t > \sim 2.2 \text{ T}$). Another problem is assist of plasma current start-up by EC. The available toroidal electric field E_ϕ for plasma current start-up will be 0.2-0.3 V/m, and startup assist by EC will be necessary. The EC assisted start-up was demonstrated for

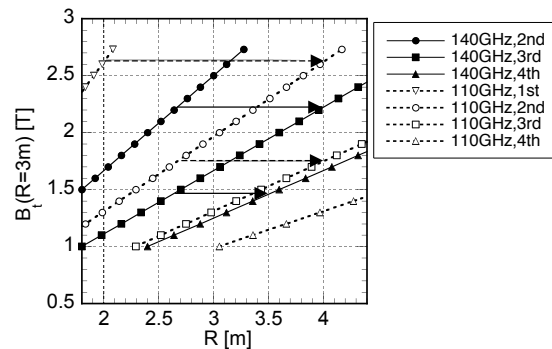


FIG. 2. Resonance radius of ECRF waves as a function of toroidal field.

fundamental and 2nd harmonic resonances, but not yet for 3rd resonance [8]. Form these two reasons, we have decided to reserve the present 110 GHz system (gyrotron magnets, wave guides and so on) for 3 MW injection and add a 140 GHz system for 4 MW injection. These two systems allow us to apply EC waves over a wide range of toroidal field.

3.2. N-NB system

The original beam lines of N-NBI pass near the equatorial plane as shown by broken lines in Fig. 3 (a). This results in a peaked profile of beam-driven current density j_{BD} , and hence the minimum value of the safety factor q_{min} less than unity even for full non-inductive CD conditions. Since $q_{min} > 1$ or suppression of sawtooth instability is believed necessary to achieve high beta and high confinement, it has been decided to shift the N-NBI beam lines downward, as shown by solid lines in Fig. 3 (a), to

obtain a broad current profile with weak/reversed magnetic shear as shown in Figs. 3 (b) and (c). The question is how much the beam lines should be lowered. In the previous design [2], the power of N-NB was 3 MW, which was only a small fraction (12%) of total beam heating power 25 MW. Furthermore, the beam current drive with positive ion NB, P-NB was also available. Hence a large vertical shift of N-NB, about 1 m, was planned [2], in which on-axis CD by P-NB and off-axis CD by N-NB were expected. In the recent design, on the other hand, the power of N-NB is 10 MW or 24% of the total heating power 41 MW. The tangential units of P-NB are now balanced, and hence the N-NB is the only source for NBCD. A large vertical shift of N-NB would cause small on-axis heating power and too broad NBCD profile.

The result on the scan of vertical position of N-NB, Z_{NNB} , is shown in Fig. 4 (a) for a lower-single-null configuration with $A = 2.8$, $\kappa_{95} \sim 1.75$, Z_{axis} (height of magnetic axis) ~ 0.07 m. The plasma current is 2.4 MA and the N-NB power is 10 MW (500 keV). The density and temperature are assumed to have smooth profiles without internal transport barrier (ITB) or edge transport barrier (ETB) and are scaled so as to have full non-inductive operation in the ACCOME [9] analysis with $\beta_N \sim 4$ and $f_{BS} \sim 70\%$ for 41 MW heating. The smooth profiles for density and temperature are employed to obtain the dependence of MHD stability limit on q_{min} , in the following analysis, without being affected by influence of change of relative position of steep pressure gradient region and the radius of q_{min} . The q_{min} increases with a larger shift of N-NB; $q_{min} \sim 1.6$ for $Z_{NNB} = -0.6$ m and ~ 2 for $Z_{NNB} = -0.9$ m. The $q_{min} > 2$ is usually employed in the design study of fusion power plants including ARIES-RS [10], ARIES-AT [11] and CREST [12] due to high MHD stability.

A steady-state operation scenario for ITER also assumes $q_{min} > 2$ [13]. The stability of these full

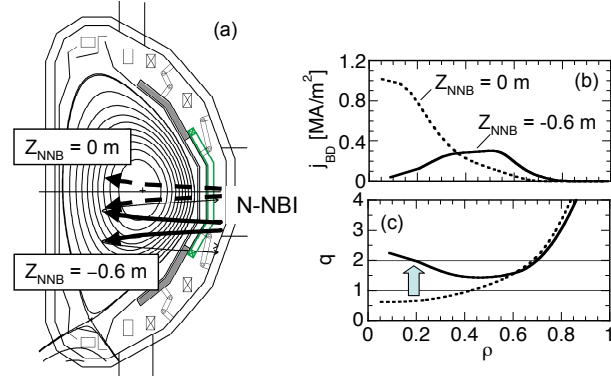


FIG. 3. Shift of N-NB position and its effects on current and q profiles.

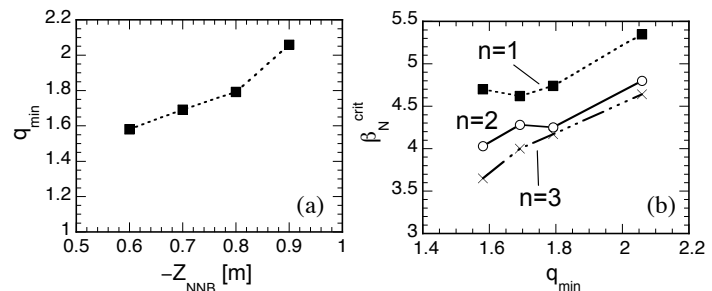


FIG. 4. (a) Dependence of q_{min} on the N-NB position Z_{NNB} . (b) Ideal beta limit for $n = 1, 2, 3$ modes as a function of q_{min} .

CD plasmas has been analyzed with MARG2D code [14] for $n = 1, 2, 3$ ideal kink-ballooning modes, where n is the toroidal mode number. The results are shown in Fig. 4 (b) for a conformal ideal wall located at $r_w/a = 1.3$. Here, r_w denotes the wall radius. The ideal wall limit increases with q_{\min} and is given by the $n=3$ mode. The no-wall limit also increase with q_{\min} , but is given by the $n=1$ mode.

The above results indicate that a large shift, $Z_{\text{NNB}} \sim -0.9$ m, is preferable in viewpoint of MHD stability. On the other hand, small central heating power accompanied with a large shift may result in degraded energy confinement especially in a high-density regime. Figure 5 shows the beam power deposition profile for a high-density plasma ($n_e\text{-bar} = 9.8 \times 10^{19} \text{ m}^{-3}$) with a configuration shown in Fig. 1 (b). The power deposition of P-NB is very hollow. The power deposition of N-NB is peaked even in this high-density regime if its present position is maintained ($Z_{\text{NNB}} = 0$), while its peak moves outward as the N-NB position is moved downward. The profile for the 0.9 m shift seems to be too hollow. Considering the MHD stability and central heating, the shift of 0.6 m is taken as a standard point for the present design. Note that far off-axis current drive for achieving $q_{\min} \sim 2$ is possible by using a USN configuration with its magnetic axis elevated, while near on-axis heating is also possible by using a LSN configuration with the axis lowered.

4. RWM control

The values of β_N that are aimed to sustain in JT-60SA, $\beta_N = 3.5\text{-}5.5$, are believed to exceed the no-wall beta limit, in particular for a weak or reversed magnetic shear plasma that will be employed for full non-inductive operation with a large fraction of bootstrap current. Hence stabilization of ideal kink modes by a conducting wall is needed. The wall with finite conductivity increases the growth times of kink modes to the time scale for decay of eddy currents in the wall. The resulting slowly growing instabilities, called resistive wall modes (RWMs), have to be stabilized by plasma rotation or active feedback control. Effects of plasma toroidal rotation on RWM will be studied by using co and counter tangential units of P-NB. We will prepare non-axisymmetric coils outside the vessel, on the surface of cryostat for instance, to reduce slowly varying error fields and enhance the controllability of plasma rotation. The largest source of error fields will be field corrections coils for shielding ion sources of P-NB from stray field from the poloidal field coils. A stabilizing plate and active feedback control coils (sector coils) are prepared for the RWM control. The growth rates of RWM are evaluated by the VALEN code [15] with three dimensional actual geometry of stabilizing plate and sector coils.

In the previous design, the sector coils were located on the outer side of the stabilizing plate and the achievable β_N (β_N^{crit}) was not so high (3.8) [16]. A later analysis indicated that β_N^{crit} can be improved significantly (5.6), close to the limit with the ideal conducting wall, for the sector coils on the inner side of the stabilizing plate. This indicates that sufficient coupling between sector coils and the

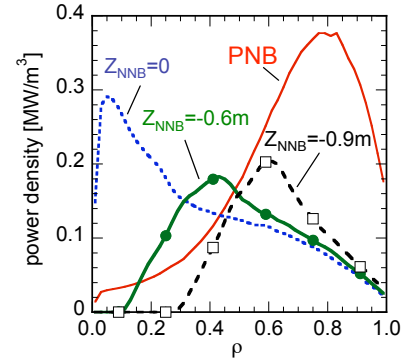


FIG. 5. Power deposition profiles for P-NB (24 MW, 85 keV) and N-NB (10 MW, 500 keV) in a high-density plasma.

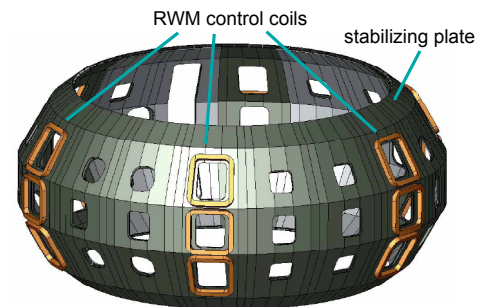


FIG. 6. RWM control coils.

plasma is important for RWM control. In the present design, sector coils are located on the outer sides of the stabilizing plates along the edge of large port holes for efficient coupling as shown in Fig. 6. The poloidal arrays of three coils are distributed nearly every 60 degrees in the toroidal angles, and hence we have 18 coils. Each coil will have a current of 20 kAT, which will generate 1 G (10^{-4} T) of $m=3, n=1$ component of radial magnetic field. We are also able to have $n=2$ components. The result of VALEN analysis for $n=1$ modes is shown in Fig. 7. The plasma aspect ratio is $A = 2.8$ and the wall is located at $r_w/a = 1.3$ on the outer equatorial plane. The pressure and current profiles consistent with the ACCOME analysis are employed, where $q_{\min} \sim 2.1$. The high beta value $\beta_N = 4.3$ is expected, which is close to the ideal wall limit ($\beta_N^{\text{ideal-wall}} = 4.42$), while the no-wall limit is $\beta_N^{\text{no-wall}} = 2.56$. Hence $C_\beta = (\beta_N - \beta_N^{\text{no-wall}}) / (\beta_N^{\text{ideal-wall}} - \beta_N^{\text{no-wall}}) = 0.9$ and very efficient RWM stabilization is expected.

5. Evaluation of operation regimes

5.1. High-beta full non-inductive operation

Sustainment of a high β_N (3.5-5.5) full non-inductive CD plasma for more than 100 s is one of the main missions of JT-60SA. The upgraded heating power has extended the operation regime for full current drive as shown in Fig. 8. Here, a low-aspect-ratio configuration with $A = 2.65$ and a shift of 60 cm of N-NB ($Z_{\text{NNB}} = -0.6$ m) is assumed. The density and temperature profiles are assumed to have both ITB and ETB as shown in Fig. 8 (c). A full CD operation with a high normalized density of $\bar{n}_e/n_{\text{GW}} = 0.86$ ($\bar{n}_e = 4.9 \times 10^{19} \text{ m}^{-3}$) is possible at $I_p = 2.4$ MA for $\text{HH}_{y2} = 1.33$ and total power of 41 MW. Figure 7 (c) shows profiles of the 2.4 MA case ($B_t = 1.79$ T, $q_{95} = 5.5$, $\beta_N = 4.4$, $\beta = 5.0\%$). The fraction of the bootstrap current ('BS') is $f_{\text{BS}} = 0.70$. The resultant q profile has a broad weak shear region with $q_{\min} \sim 1.5$. The values of

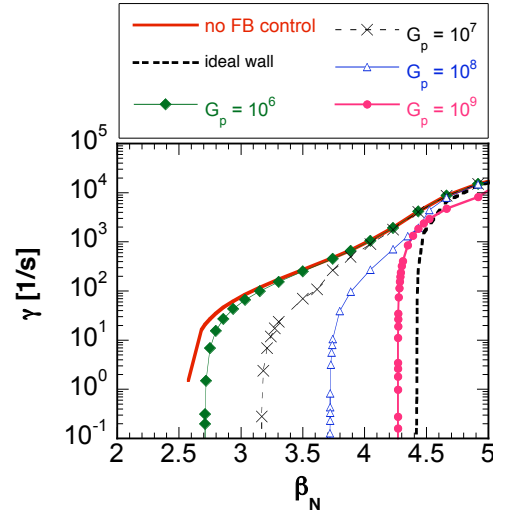


FIG. 7. Growth rate of RWM as a function of β_N for different proportional gain G_p of RWM control including the ideal wall case and no feedback control case.

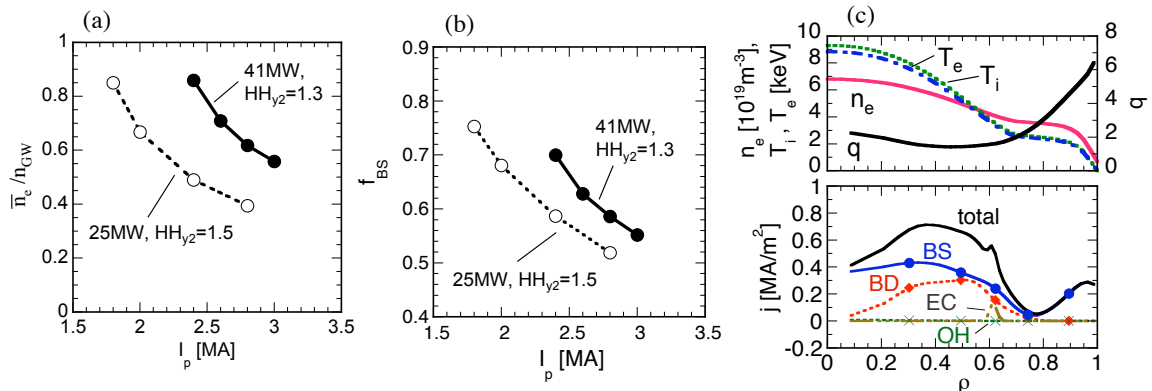


FIG. 8. Extended region of full non-inductive current drive with increased heating power. (a) The density normalized with the Greenwald density and (b) the bootstrap current fraction as a function of plasma current. (c) Profiles of n_e , T_e , T_i , q and current densities for a 2.4 MA full CD plasma.

A , q_{95} , κ , β_N , β , HH_{y2} and f_{BS} are very close (within 10%) to those in a DEMO design with a slim center solenoid proposed by JAEA [17, 18]. A full CD plasma with $I_p = 3$ MA ($\beta_N = 3.7$, $f_{BS} = 0.55$) is also possible with reduced \bar{n}_e/n_{GW} of 0.56 for $HH_{y2} = 1.31$. Note that $HH_{y2} = 2$ was required to obtain a 3 MA full CD plasma for the previous 25 MW case [3]. Though the density and temperature profiles are assumed and fixed in shape in this study, the value of f_{BS} attained with $HH_{y2} = 1.33$ does not strongly depend on the assumed profiles; $f_{BS} = 0.67$ - 0.73 for $p(0)/\langle p \rangle = 2.1$ - 3.4 and $n_e(0)/\langle n_e \rangle = 1.4$ - 2.5 .

5.2. High density ELMy H-mode operation

One of the reasons for upgrade of heating power is for high-density operation. The threshold power P_{th} for the L to H transition is one of the key parameters for high-density experiment, since it increases nearly linearly with the density. Figure 9 shows P_{th} estimated by one of the scalings [19] for the grad-B drift toward the X-point as a function of the electron density normalized with the Greenwald density (n_{GW}). The previous value of heating power (25 MW) was marginal for high-current (5.5 MA), high-density ($n_e/n_{GW} = 0.85$ - 1) plasmas. The enhanced heating power of 41 MW will be sufficient to maintain high confinement ($HH_{y2} \sim 1$) ELMy H-mode in the high-density regime. Improved H-mode with higher confinement ($HH_{y2} > \sim 1$) is also expected, which requires heating power larger than $2P_{th}$ in ASDEX Upgrade [20]. On the other hand, the density for full CD operation described in the previous section is 4 - $5 \times 10^{19} \text{ m}^{-3}$, which results in P_{th} of about 10 MW. The direction of the toroidal field should be fixed to co or counter to the plasma current in order to avoid the leading edge problem of divertor target. Either upper or lower divertor is opposite to the grad-B drift direction, in which P_{th} is increased about 50%. The P_{th} will be ~ 15 MW even for the grad-B drift away from the X-point. Hence the nominal direction of toroidal field will be in the clock-wise direction with the grad-B drift downward.

Enhanced heating power has also enabled high beta operation in high density H-mode. In an ITER-like plasma shape with $A = 3.1$, high β_N (3.1) ELMy H-mode plasmas with an ITER-relevant high density ($\bar{n}_e = 9.1 \times 10^{19} \text{ m}^{-3}$, $\bar{n}_e/n_{GW} = 0.85$) are expected at $I_p = 3.5$ MA and $HH_{y2} = 1.1$. The experiment in this regime will contribute to optimization of ITER operation scenarios for improved H-mode or 'hybrid' mode.

Since the α particles generated by DT fusion reaction mainly heats electrons rather than ions, electron heating power is dominant in ITER and DEMO reactors. The enhanced power of N-NB and ECRF contributes to increase the electron heating power as shown in Fig. 10. A large fraction of electron heating power ($\sim 65\%$) is obtained for the full power heating case. The fraction equal to that

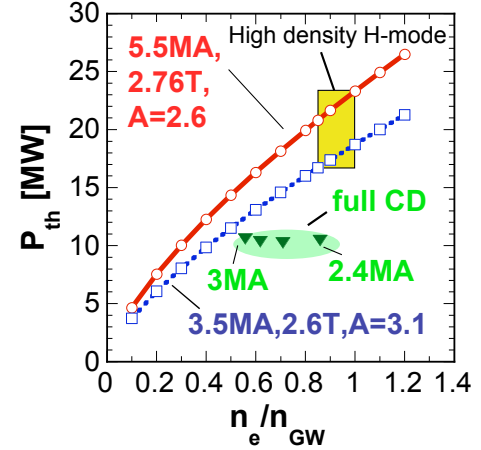


FIG. 9. The threshold power for L to H transition as a function of the density normalized with the Greenwald density.

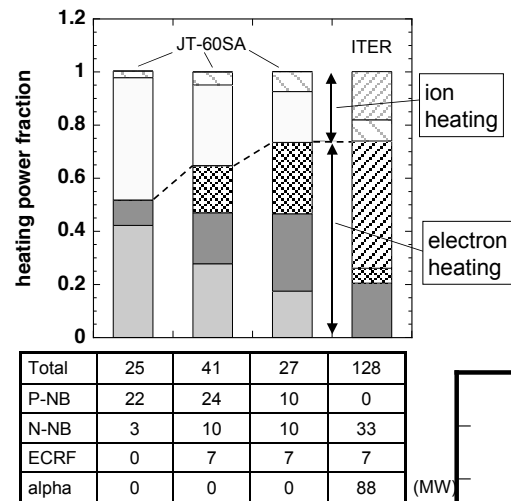


FIG. 10. Fraction of ion and electron heating power.

in ITER, 74%, is also possible with reduced power of 27 MW.

The power and particle controllability is an important issue for the enhanced heating power. The analysis on a DN configuration with the B2-Eirene code indicates that 70-80% of power is concentrated to the divertor on the 1st X-point side if the 2nd X-point is located on the 5 mm SOL field line. In the single-null configuration, the maximum heat flux density to the outer target is reduced from ~ 16.5 MW/m² to ~ 11 MW/m² by intense gas-puff rate of 3×10^{22} /s even the for full heating power case. Study on controllability of high density plasmas, including the effects of impurities is in progress.

6. Summary

Design on some components in JT-60SA including poloidal field coils, divertor and first wall, RWM control coils, ECRF and N-NB systems, have been optimized for plasma control toward high beta steady-state operation. As a result, an additional equilibrium field coil, different geometry for up and down divertors, two frequencies ECRF, lowered beam line of N-NB, RWM coils along the port hole, have been decided. The operational regime has been evaluated with the enhanced heating power of 41 MW including 10 MW of N-NB and 7 MW of ECRF. High beta full non-inductive current drive is possible for the plasma current of 2.4 to 3 MA. High density high beta ELMy H-mode operation with ITER-like configuration is also possible at 3.5 MA.

Acknowledgement

The authors express their thanks to the JT-60SA design team, the staff of JAEA and researchers in universities for useful discussions and continuous supports.

References

- [1] TAMAI, H., et al., Nucl. Fusion **45** (2005) 1676.
- [2] KIKUCHI, M., et al., Nucl. Fusion **46** (2006) S29.
- [3] KIKUCHI, M., et al., FT/2-5, this conference.
- [4] MATSUKAWA, M., et al., FT/P7-5, this conference.
- [5] WADE, M.R., et al., Phys. Plasmas **8** (2001) 2208.
- [6] FERON, J.R., et al., Phys. Plasmas **7** (2000) 1976.
- [7] SAKURAI, S., et al., "Design of plasma facing component for JT-60SA", in 24th SOFT Conf. (2006).
- [8] KAJIWARA, K., et al., Nucl. Fusion **45** (2005) 694.
- [9] TANI, K, AZUMI, M., DEVOTO, R.S., J. Comp. Phys. **98** (1992) 332.
- [10] JARDIN, S. C., et al., Fusion Eng. Design **38** (1997) 27.
- [11] KESSEL, C.E., et al, Fusion Eng. Design **80** (2006) 63.
- [12] OKANO, K., et al., Nucl. Fusion **40** (2000) 635.
- [13] POLEVOI, A.V., et al, 2002 Proc. 19th Int. Conf. on Fusion Energy 2002 (Lyon, 2002) (Vienna: IAEA) CD-ROM file CT/P-08.
- [14] TOKUDA, S., WATANABE, T., Phys. Plasmas **6** (1999) 3012.
- [15] BIALEK, J. et al., Phys. Plasmas **8** (2001) 2170.
- [16] KURITA, G., et al., Nucl. Fusion **46** (2006) 383.
- [17] TOBITA, K., et al., Fusion Eng. Design. **81** (2006) 1151.
- [18] TOBITA, K, et al., FT/P5-22, this conference.
- [19] TAKIZUKA, T., et al., Plasma Phys. Control. Fusion **46** (2004) A227.
- [20] GIANNONE, L., et al., Plasma Phys. Control. Fusion **46** (2004) 835.